Long-range retarded elastic metamaterials: wave-stopping, negative and hypersonic/superluminal group velocity

A. Carcaterra,* F. Coppo, F. Mezzani, and S. Pensalfini
Department of Mechanical and Aerospace Engineering, Sapienza University of Rome
(Dated: 2nd January 2019)

This paper investigates new phenomena in elastic wave propagation in metamaterials, characterised by long-range interactions. The kind of waves borne in this context unveil wave-stopping, negative group velocity, instability and hypersonic or superluminal effects, both for instantaneous and for nonlocal retarded actions. Closed form results are presented and a universal propagation map synthesizes the expected properties of these materials. Perspectives in physics, engineering and social dynamics are discussed.

Keywords: elastic metamaterials; long-range interaction; wave propagation; negative group velocity; hypersonic/superluminal group velocity

I. INTRODUCTION

Metamaterials are known to yield unexpected results in many applications. For example, in electromagnetics these are frequently related to anomalous refraction index and dissipation. Studies have demonstrated unusual wave propagation [1] by synthesizing negative group velocity, or light stopping [2–5], or fast light, using special dissipation and diffraction properties of electromagnetic media [6–9]. Even an acoustic setup has been proposed in [10], where, with electronically assisted devices, wave trains of desired spectral composition and superluminal wave propagation have been observed [11]. Waves in plasmas and charged gases also represent a stimulating example of acoustic fields controlled by long-range electrical interactions [12–15]. In mechanics, metamaterials introduced micropolar, higher-gradient and nonlocal elasticity [16–24].

In one of the rare investigations of nonlocal dispersion relationship [20], the author identifies the long-range elastic modulus, based on Brillouin dispersion in a lattice [25], that he compares successfully with experimental results [26]. Even in the landscape of recent investigations of elastic metamaterials, the correlation between waves and nonlocality is not directly addressed [27] and the scientific literature does not report results on anomalous elastic wave propagation analogous to those found in electromagnetics. Even though nonlocal interactions have been investigated in several areas [20, 28–32], the lack of general results for dispersive properties in nonlocal materials should not be surprising since theoretical investigations in this field suggest complex integral-differential equations in space and differential in time to describe the wave propagation. In the present paper, the dispersion relationship is analytically determined for elastic materials with long-range and retarded constitutive relationships yielding surprising wave propagation behaviors, namely wave-stopping, negative and hypersonic or superluminal group velocity, as a direct effect of nonlocality.

Dissipation effects are also included in the model, but it is shown they do not represent a necessary condition to produce superluminal propagation. The derivations presented here allow discussion in detail of the wave propagation scenarios, related to the elastic long-range interactions, unveiling the unexpected effects previously mentioned. The approach used here considers long-range interactions by examining their connectivity characteristics. Unlike in classical waves, which are borne out of particle-particle connections between the closest neighbors, unconventional effects result when one-to-all particles connections are introduced, as in [33–38], and when all-to-all connections appear, as in Vlasov's theory [39] or in quantum physics [40, 41], or in the case of elastic materials investigated here.

The mechanism for wave-stopping, negative group velocity and hypersonic (superluminal) propagation illustrated in this paper is demonstrated by simple long-range forces. The particle-particle interaction forces in this case rapidly decay with the distance and asymptotically vanish, as in many physical forces, namely electrostatic, magnetostatic or gravitational. These interaction forces are represented in this paper with two families of exponentially decaying functions, the Gauss-like and the Laplace-like, which lead to expressions for dispersion relationships. Three regimes of interactions are demonstrated, according to the distance range and the intensity of the force, quantified by the long-range elastic modulus E^*: (i) negative group velocity and wave-stopping, (ii) hypersonic (superluminal) group velocity and instability, (iii) eigenstates migration.

The existence of hypersonic or superluminal waves stimulated additional investigation of the retarded long-range actions. It is shown that, even when a particle-particle interaction is retarded because of its finite speed v_f, the group velocity can still be hypersonic (superluminal), even with negative group velocity and the phase speed can overcome the upper bound v_f as well.

These effects are investigated in authoritative works by Brillouin, Sommerfeld and Voigt (see [42] and citations therein) that show they fit the framework of relativity,

* Corresponding Author. E-mail: antonio.carcaterra@uniroma1.it

since group and phase velocities do not coincide with the signal velocity, which indeed remains always confined below the upper bound of the speed of light.
The terms hypersonic and superluminal denomination are used in this paper for sound or light, respectively, to indicate very fast waves that can exceed the phase or group velocity of sound or light, respectively, depending on the nature of the D'Alembert waveguide and on the value of v_f.

II. EQUATION OF MOTION

In this section, we analyse the case of long-range force, additional with respect to the classical elastic interaction. We define $\mathbf{F}(\boldsymbol{P},\boldsymbol{Q})$ as the force borne on the particle at $\boldsymbol{P}$, because of the particle at $\boldsymbol{Q}$ (Figure 1). $\mathbf{F}$ should guarantee the action-reaction principle holds:

$$\mathbf{F}(\boldsymbol{P},\boldsymbol{Q}) = -\mathbf{F}(\boldsymbol{Q},\boldsymbol{P}). \tag{1}$$

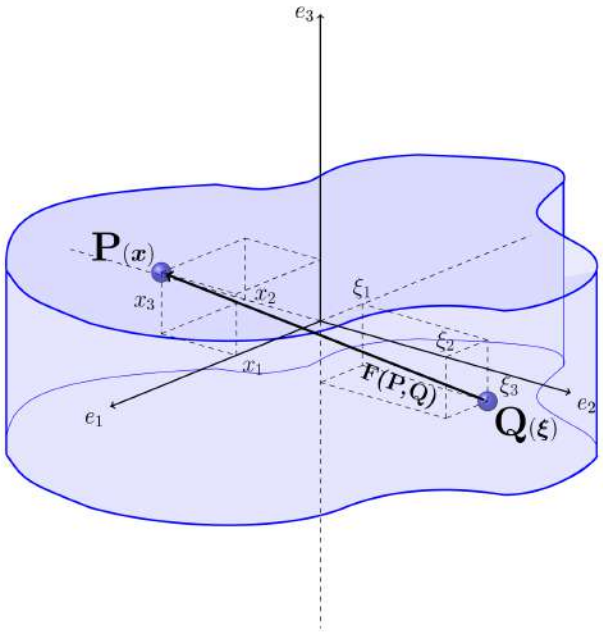

Figure 1: Sketch of long-range interaction.

The force between two material elements, in the initial reference configuration at $\boldsymbol{x}$ and $\boldsymbol{\xi}$, respectively, can be expressed as:

$$\mathbf{F}\left(\boldsymbol{x}+\boldsymbol{u}(\boldsymbol{x},t),\boldsymbol{\xi}+\boldsymbol{u}(\boldsymbol{\xi},t)\right) = -f(|\mathbf{r}|)\mathbf{r} \tag{2}$$

where

$$\mathbf{r} = \boldsymbol{x}-\boldsymbol{\xi}+\mathbf{u}(\boldsymbol{x},t)-\mathbf{u}(\boldsymbol{\xi},t) \tag{3}$$

with $\mathbf{u}(\boldsymbol{x},t)$ the displacement in the elastic medium and with the convention introduced by equation (2), it follows $f(|\mathbf{r}|)$ is negative for repulsive force, and positive for the attractive case.
Forces decaying with $|\mathbf{r}|$, such that $\lim_{|\mathbf{r}|\to\infty} f(|\mathbf{r}|)\mathbf{r} = 0$, are here considered. This property is typical, for example, of magnetostatic, Coulomb and gravitational forces.
Long-range characteristic leads to nonlinear integral-differential equations to control the wave propagation. Starting from the Navier-Cauchy formulation, for a continuous unbounded three-dimensional elastic solid, we obtain:

$$\rho\,\mathbf{u}_{tt}(\boldsymbol{x},t) - \frac{E}{2(1+\nu)}\left[\nabla^2\mathbf{u}(\boldsymbol{x},t) + \frac{1}{1-2\nu}\nabla\left(\nabla\cdot\mathbf{u}(\boldsymbol{x},t)\right)\right] + \int_{\boldsymbol{\xi}\in\mathbb{R}^3} f(|\mathbf{r}|)\mathbf{r}\;dV = 0 \tag{4}$$

with ρ, E and ν the density, the Young modulus and the Poisson ratio of the medium, respectively and ∇ the Laplace operator.
The integral represents the sum of non-conventional long-range forces and the focus of the present paper.
For acoustic media with long-range interactions (the case of electrostatic approximation of low frequency plasma [43]) the equation of motion can be simplified as $\square\, u(\boldsymbol{x},t) + \int_{\boldsymbol{\xi}\in\mathbb{R}^3} f(|\mathbf{r}|)\mathbf{r}\;dV = 0$. In general, analytic solutions are not possible. However, the linearization of the force $f(|\mathbf{r}|)$, with respect to $\boldsymbol{\varepsilon} = \mathbf{u}(\boldsymbol{x},t) - \mathbf{u}(\boldsymbol{\xi},t)$ and for small deformation, permits, together with some additional hypotheses introduced later, to investigate closed form solutions, providing important insights into the wave propagation properties.
Taylor series of the force up to the first order in terms of $\boldsymbol{\varepsilon}$ is:

$$f(|\mathbf{r}|)\mathbf{r} \sim (\boldsymbol{x}-\boldsymbol{\xi})\,f_0 + \boldsymbol{h}_0\boldsymbol{\varepsilon} + f_0\boldsymbol{\varepsilon} \tag{5}$$

where

$$f_0 = f\left(|\boldsymbol{x}-\boldsymbol{\xi}|\right) \tag{6}$$

$$\boldsymbol{h}_0 = \left.\frac{\partial f}{\partial|\boldsymbol{r}|}\right|_0 \frac{(\boldsymbol{x}-\boldsymbol{\xi})\otimes(\boldsymbol{x}-\boldsymbol{\xi})}{|\boldsymbol{x}-\boldsymbol{\xi}|} \tag{7}$$

and the subscript 0 denotes quantities evaluated at $\boldsymbol{\varepsilon} = \mathbf{0}$ and $\otimes$ is the tensor product operator.
Therefore, the linearized integral term of equation of motion (4) becomes:

$$\int_{\boldsymbol{\xi}\in\mathbb{R}^3} \left[(\boldsymbol{x}-\boldsymbol{\xi})\,f_0 + \boldsymbol{h}_0\boldsymbol{\varepsilon} + f_0\boldsymbol{\varepsilon}\right] dV \tag{8}$$

Separation of the static and the dynamic components of the displacement, $\mathbf{u}(\boldsymbol{x},t) = \mathbf{v}(\boldsymbol{x}) + \mathbf{w}(\boldsymbol{x},t)$, leads to:

$$\rho\mathbf{w}_{tt} + \frac{E}{2(1+\nu)}\left[\nabla^2\mathbf{w} - \frac{1}{1-2\nu}\nabla\left(\nabla\cdot\mathbf{w}\right)\right] + \bar{\boldsymbol{h}_0}\cdot\mathbf{w} - [\boldsymbol{h}_0 * \mathbf{w}] + \bar{f_0}\mathbf{w} - [f_0 * \mathbf{w}] = 0 \tag{9}$$

for the dynamic component, where $\bar{\cdot}$ indicates average over $\mathbb{R}^3$ and $*$ indicates the convolution operator.
In this wave-dynamics context, we are not interested in the discussion of $\mathbf{v}(\boldsymbol{x})$. Indeed, for those forces that obey:

$$\int_{\boldsymbol{\xi}\in\mathbb{R}^3} (\boldsymbol{x}-\boldsymbol{\xi}) f_0 \, dV = 0 \tag{10}$$

$\mathbf{v}(\boldsymbol{x})$ vanishes and $\boldsymbol{w}(\boldsymbol{x},t)$ remains the only displacement field, the case we consider ahead.
Moreover, for special choices of the function $f(|\boldsymbol{r}|)$, equation (9) can exhibit analytical solutions, as illustrated in the following sections.

III. ONE-DIMENSIONAL WAVEGUIDE

The one-dimensional version of (9) is analysed, introducing the Gauss-like and the Laplace-like forces (see equations (15) and (18)), for which it simplifies as:

$$\rho\frac{\partial^2 w}{\partial t^2} - E\frac{\partial^2 w}{\partial x^2} - g(x) * w(x) = 0 \tag{11}$$

where $g(x) = h_0(x) + f_0(x)$ and these cases $\bar{h_0} = 0$ and $\bar{f_0} = 0$. Since for the aforementioned interaction forces, $g(x) = -\frac{\partial F(x)}{\partial x}$, equation (11) becomes:

$$\rho\frac{\partial^2 w}{\partial t^2} - E\frac{\partial^2 w}{\partial x^2} + F(x) * \varepsilon_x = 0 \tag{12}$$

where ε_x is the strain along the axis, a form consistent with the Eringen formulation for nonlocal elasticity in $1D$ [20].
Assuming:

$$w(x,t) = \iint_{-\infty}^{+\infty} W(k,\omega) e^{j(kx-\omega t)} dk \, d\omega \tag{13}$$

or taking the Fourier transform $\mathcal{F}\{\cdot\}$ of (11) with respect to x and t, the dispersion relationship is obtained:

$$\rho\omega^2 - Ek^2 + G(k) = 0 \tag{14}$$

where $G(k) = \mathcal{F}\{g(x)\}$. Gauss-like and Laplace-like forces unveil some general properties of long-range interaction. These forces present three advantages: (i) they guarantee the action-reaction principle holds, (ii) they vanish for large x, a typical property of some long-range forces met in physics and (iii) they admit an analytical known Fourier transform $G(k)$.

A. Gauss-like interaction

The Gauss-like form is:

$$f(r) = \mu e^{-\left(\frac{r}{\beta}\right)^2} \tag{15}$$

where μ controls the intensity of the force and β (positive) is the interaction length. The sign of μ follows the convention stipulated in section II: μ can be positive or negative, to represent attractive or repulsive actions, respectively. Moreover, $F(r) = -F(-r)$ and $\lim_{r\to\infty} F(r) = 0$. Combining equations (15) and (11):

$$\rho\frac{\partial^2 w}{\partial t^2} - E\frac{\partial^2 w}{\partial x^2} - \mu\int_{-\infty}^{+\infty}\left(1-\frac{2}{\beta^2}\xi^2\right)e^{-\left(\frac{r}{\beta}\right)^2} w(x-\xi)d\xi = 0. \tag{16}$$

For the Gauss-like force, $G(k) = \frac{\mu\beta^3}{2\sqrt{2}}k^2 e^{-\frac{\beta^2k^2}{4}}$ and

$$\Omega = \pm K\sqrt{1-\chi e^{-\frac{K^2}{4}}} \tag{17}$$

is the dispersion relation associated to (16), where $\Omega = \sqrt{\frac{\rho}{E}}\beta\omega$, $K = \beta k$, and $\chi = \frac{\mu\beta^3}{2\sqrt{2}E}$ are nondimensional parameters.
χ is a scale factor that relates the intensity of the long-range interaction in terms of its elastic modulus $E^* = \frac{\mu\beta^3}{2\sqrt{2}}$ (positive or negative) and the elastic modulus E.
As for μ, the sign of χ controls the attraction ($\chi > 0$) or repulsion ($\chi < 0$) characteristic of the force.
Note that equation (17) can produce, for some wavenumber and χ ranges, imaginary values. This implies the waveguide becomes unstable with unbounded wave amplitudes. This happens for long-range forces of negative equivalent stiffness larger than the classical elastic one.

B. Laplace-like interaction

In this case, f is based on the *Laplace Distribution*:

$$f(r) = \mu e^{-\frac{|r|}{\beta}} \tag{18}$$

with $F(r) = -F(-r)$ and $\lim_{r\to\infty} F(r) = 0$.
For $G(k) = \frac{2\sqrt{\frac{2}{\pi}}\beta^3k^2\mu}{\left(1+\beta^2k^2\right)^2}$, the associated dispersion relationship is:

$$\Omega = \pm K\sqrt{1-\frac{8\chi}{\sqrt{\pi}\left(K^2+1\right)^2}} \tag{19}$$

C. Notes on the linear approximation

The linearised approximation, discussed in section II, implies equation (9), and consequently equation (11), is valid under the assumption: $|\varepsilon| \ll |x-\xi|$. Since $\frac{|\varepsilon|}{|x-\xi|} = \frac{|w(x,t)-w(\xi,t)|}{|x-\xi|} \ll 1$, i.e. the strain is

small, at least of order 10^{-1}. A wave perturbation travels in the system as $w(x,t) = w_0 e^{j(kx-\omega t)}$. The strain is $\frac{\partial w}{\partial x} = jkw_0 e^{j(kx-\omega t)}$ and the linearisation is valid if: $\left|\frac{\partial w}{\partial x}\right| \ll 1$, hence $|w_0 k| \ll 1$. In terms of the nondimensional wavenumber $K = \beta k$, it finally produces: $\left|\frac{w_0 K}{\beta}\right| \ll 1$ and $K \ll \frac{\beta}{w_0}$.
This shows that, once the regime for K has been selected (as in the following sections), the amplitude of vibration must be compared with the characteristic interaction length β to guarantee linearisation conditions hold.
In the following sections, it appears that for $K \to \infty$, the propagation characteristic collapses into the standard D'Alembert equation. Therefore, the most typical and interesting aspect of our investigation (wave-stopping and hypersonic velocity) emerge at K of order ~ 1, i.e. the studied effects fall in the linearisation approximation when the vibration amplitude is much smaller than the characteristic long-interaction length β: $w_0 \ll \beta$.

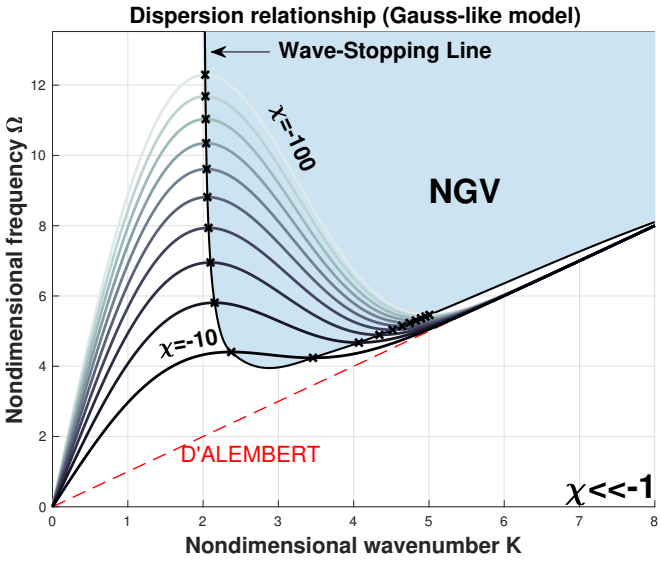

Figure 2: Dispersion curves for the Gauss-like model for different $\chi \ll -1$.

IV. WAVE SPEED

The propagation behaviour in terms of χ is discussed, which only affects the dispersion equations (17) and (19). From them, with the speed of sound $c = \sqrt{\frac{E}{\rho}}$, analytical forms follow for the group and phase velocity $C_g = \frac{1}{c}\frac{\partial \omega}{\partial k} = \frac{d\Omega}{dK}$ and $C_\varphi = \frac{1}{c}\frac{\omega}{k} = \frac{\Omega}{K}$, respectively, as well as for the eigenstate density $\frac{dN}{d\Omega} \propto \frac{1}{C_g}$.
Three ranges for χ are discussed: (i) $\chi \ll -1$, (ii) $-1 < \chi < 1$ and (iii) $\chi \gg 1$.

A. Gauss-like

1. *Negative group velocity (NGV) and wave-stopping, $\chi \ll -1$*

The dispersion curves for $\chi \ll -1$ are represented in Figure 2 that shows both points of minimum and maximum, for each χ. Wave-stopping phenomena appear, since at those points the group velocity C_g vanishes (Figure 3). Moreover, the part of the curves in Figure 2 with a positive slope is related to a conventional dynamic behaviour, whilst the negative slope side leads to a negative group velocity, denoted as NGV.
In Figure 3, the group velocity is plotted versus the wavenumber. We observe: i) the existence of wavenumbers pair for which the group velocity vanishes, producing wave-stopping, ii) the presence of a bandwidth of negative values of the group velocity, iii) larger wavenumber bandwidth, for larger values of $|\chi|$.

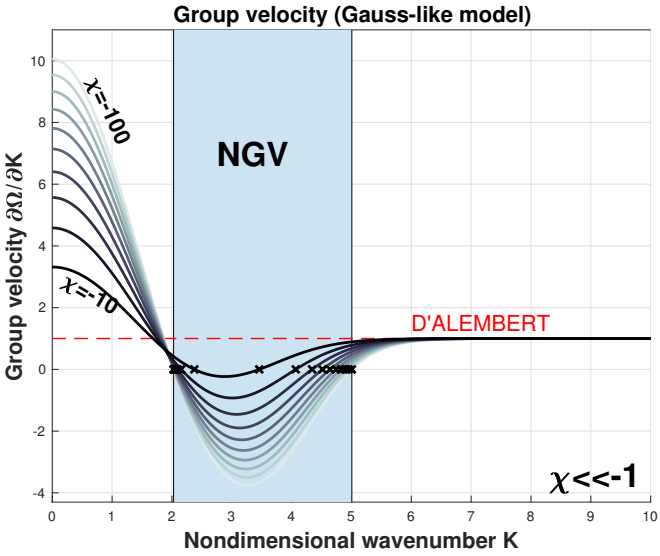

Figure 3: Group velocity for the Gauss-like model for different values of χ.

As shown in Figure 4, the phase velocity at low frequencies assumes values considerably higher if compared with a conventional waveguide, characterised by first neighbour interactions, and decreases with increasing the frequency.
Finally, Figure 5 shows the eigenstate density that exhibits two peaks. These points correspond to the vanishing group velocity.
The singularities in the eigenstate density produce an energy storage effect into the waveguide, preventing propagation and yielding the inception of wave-stopping.

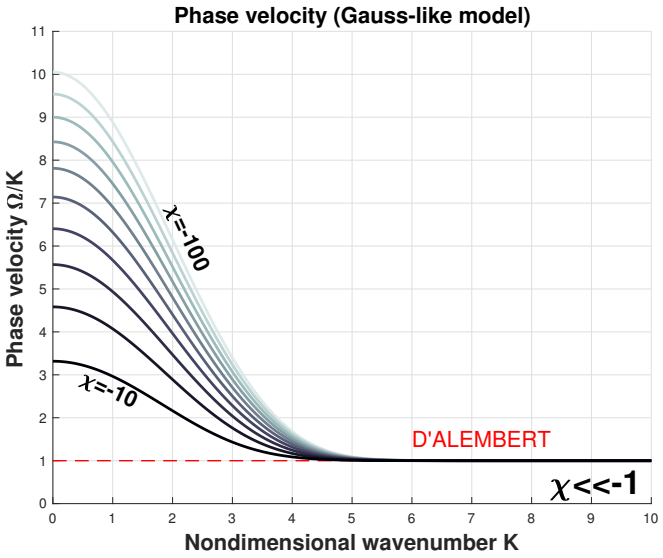

Figure 4: Phase velocity for the Gauss-like model for different values of χ.

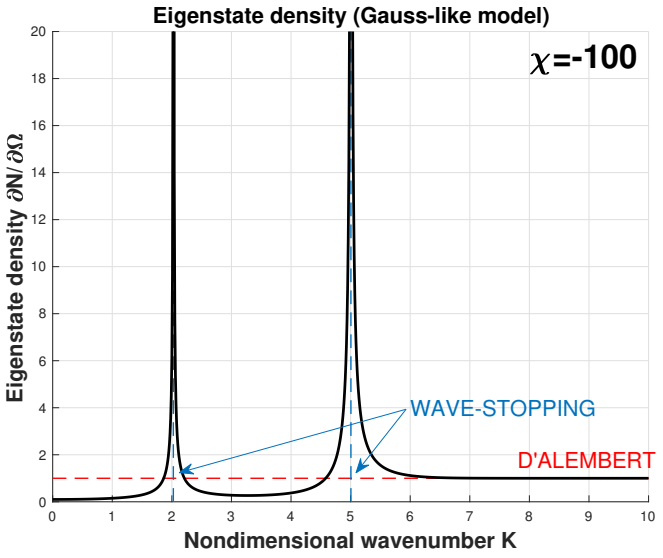

Figure 5: Eigenstate density for the Gauss-like model for different values of χ.

2. *Eigenstates migration,* $-1 < \chi < 1$

Wave dispersion phenomena are analysed in the range of χ between -1 and 1 characterised by long-range weak forces suggesting a behaviour close to the classical D'Alembert waveguide.

Figure 6a, 6b and 6c show the trend of the dispersion relationship, the group velocity and the eigenstate density, respectively. Wave-stopping effects do not occur, and the group velocity is always positive.

However, the eigenstate density, reported in Figure 6c, shows a *mode-migration* effect.

For any given χ in Figure 6c, two branches of curve

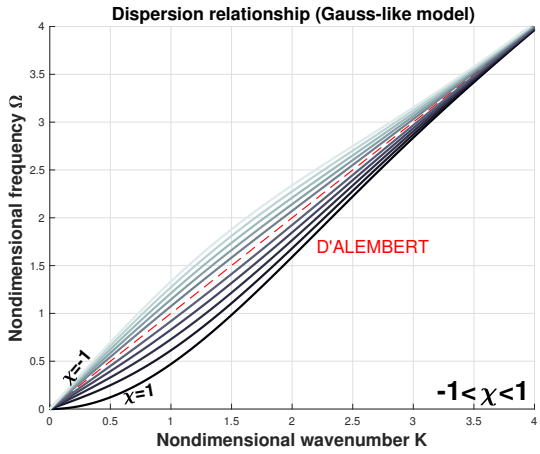

(a)

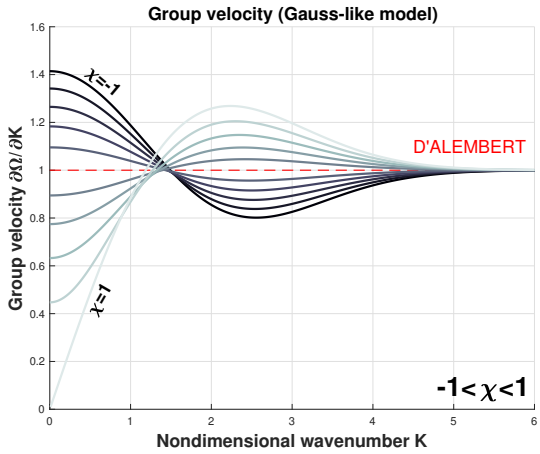

(b)

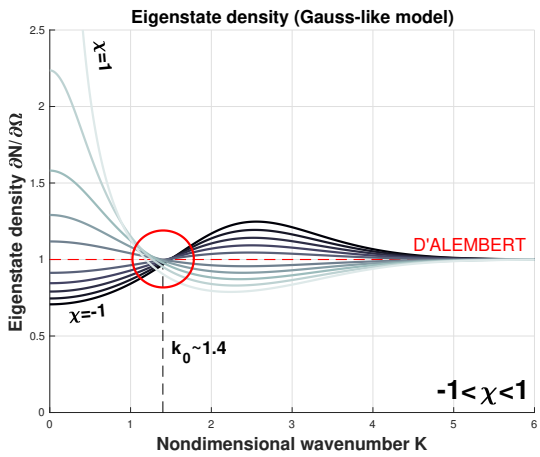

(c)

are identified: the one on the right and the one on the left with respect to the intersection with the D'Alembert curve that is at the *folding wavenumber* k_0. For example, for $0 < \chi < 1$,(Figure 6d), the left branch shows a higher eigenstate density with respect to the D'Alembert case, while the right branch a lower one. A direct inspection of

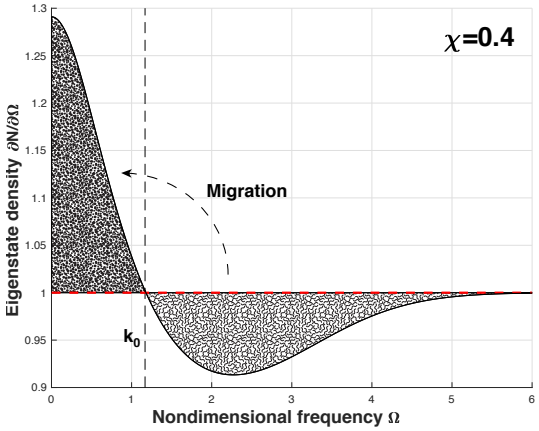

(d)

Figure 6: Dispersion curves (a), Group velocity (b), Eigenstate densities (c,d) for the Gauss-like model for $\chi \in [-1, 1]$.

the analytical expressions of the eigenstate density shows that:

$$\int_0^{k_0} \left(\frac{dN}{d\Omega} - 1 \right) d\Omega = \int_{k_0}^{+\infty} \left(1 - \frac{dN}{d\Omega} \right) d\Omega \qquad (20)$$

where $\frac{dN}{d\Omega}(k_0) = 1$. This implies that the number of the eigenstates gained by the long-range waveguide in the region $k \in [0, k_0]$ equals the number of the eigenstates lost in the bandwidth $k \in [k_0, +\infty)$. This means an eigenstate packet migrates from high to low frequency, folding about k_0. Analogous considerations hold for $-1 < \chi < 0$. For all the χ's (see Figure 6c), the characteristic value of k_0 is about 1.4.
The region characterised by a richer eigenstate density tends to trap the energy, slowing down its transport and lowering the group velocity (see Figures 6b and 6c).

3. *Hypersonic group velocity and instability, $\chi \gg 1$*

For $\chi \gg 1$, the analysis of propagation enlightens the presence of an unstable region: in it, no propagation occurs and wave amplitudes become unbounded (see Figure 7). In the propagation region, the curves start with a very high slope and the corresponding group velocity ideally becomes infinite, hence hypersonic (superluminal) group waves are borne.
The group velocity passes from the hypersonic (superluminal) to the standard D'Alembert propagation, within the wavenumber bandwidth $k \in [\sim 3, \sim 6]$.

B. Laplace-like

Dispersion relationship, phase and group velocities related to the Laplace-like force have a very similar

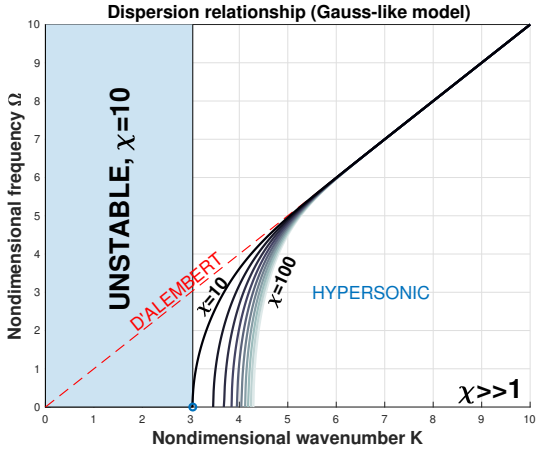

(a)

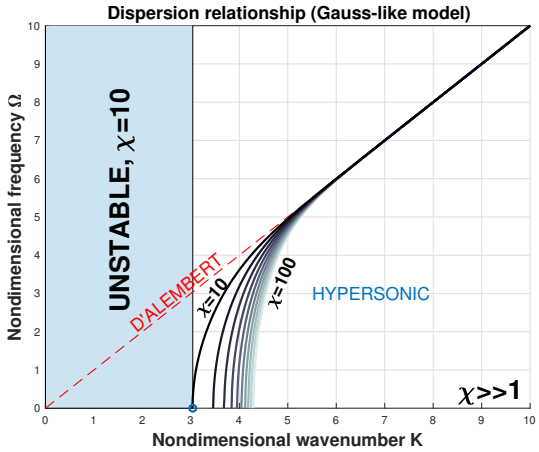

(b)

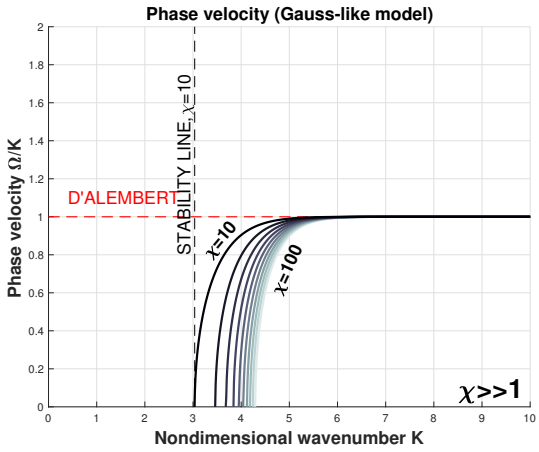

(c)

trend with respect to the Gauss-like interaction, and three identical regimes appear. This enforces the conclusion that the scenario outlined in the previous section has a general character for long-range interaction for those forces that satisfy the requirements as in section II.

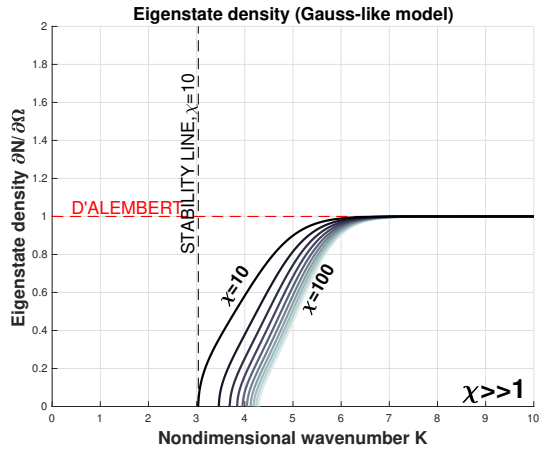

(d)

Figure 7: Dispersion curves (a), Group velocity (b), Phase velocity (c) and Eigenstate density (d) for the Gauss-like model for different values of χ.

V. SPACE-TIME VISUALISATION

Visualisation of the wave propagation in space and time corroborates the previous theoretical findings. Consistently with equation (13), waves can be represented by the discrete approximation:

$$w(x,t) = \sum_{i}^{N} \Big[W_i^{(1)} \sin\left(k_i x - \omega(k_i)t\right) + W_i^{(2)} \cos\left(k_i x - \omega(k_i)t\right) \Big] \quad (21)$$

where $W_i^{(1)}$ and $W_i^{(2)}$ are coefficients depending on initial conditions, and $\omega(k_i)$ is specified by the dispersion relationships (17) and (19). Two different graphic representations of the wave pattern are used, derived both from the surface $w(x,t)$.

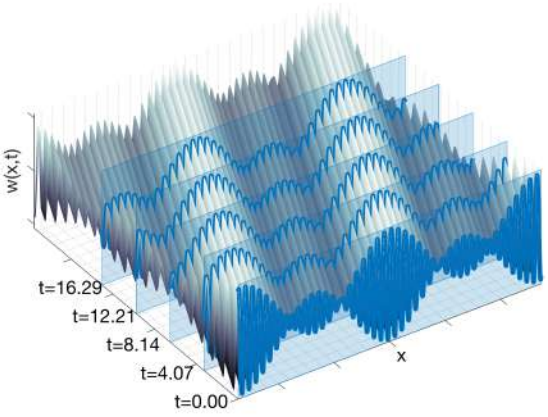

Figure 8: 3D Surface plot of the displacement.

In Figures 10, 12 and 14, sections at different times of this surface are shown, the red dot highlights the phase velocity, the green square the group velocity. Dotted lines show these points moving in space and time.

Figures 11, 13 and 15 show the surface colour plot

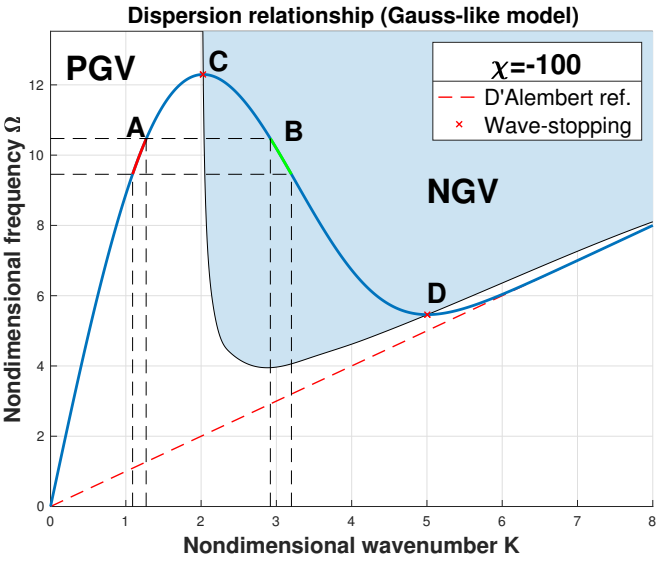

Figure 9: Selection of four arches (A,B,C,D) of the dispersion curve to generate the wavetrains shown in Figures 10-13.

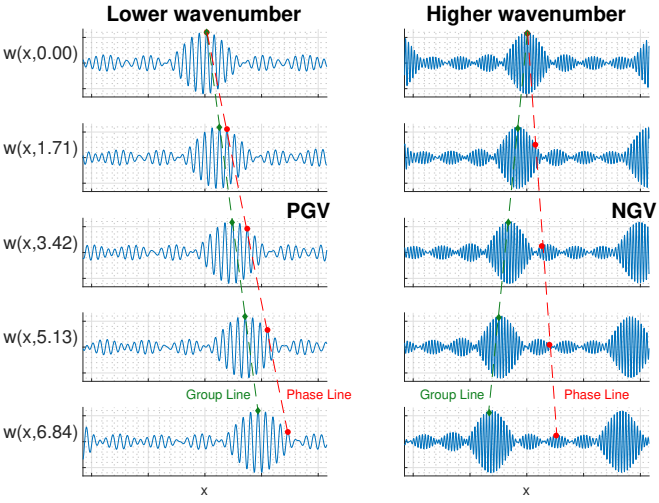

Figure 10: Left: positive group velocity, Right: negative group velocity.

of w over the x,t plane. This permits to simultaneously identify the wave characteristic lines on x,t, whose inclination remains with the phase propagation and the envelope peak regions by shaded bands, with inclination proportional to the group velocity.

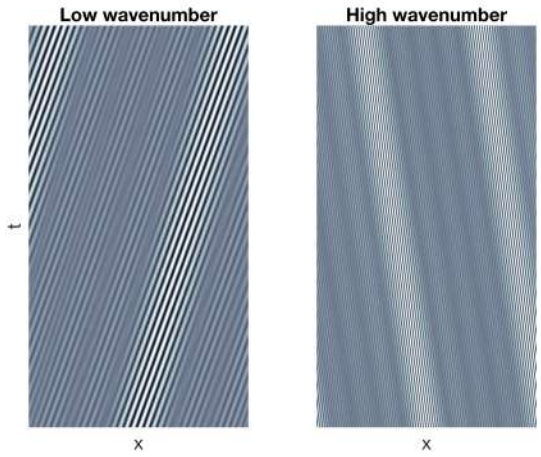

Figure 11: Surface colour plot of $w(x,t)$. Left: positive group velocity, Right: negative group velocity.

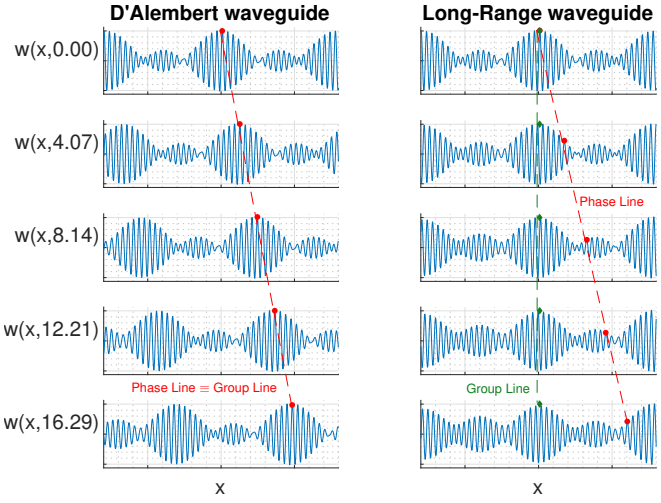

Figure 12: Wave-stopping effect. Left: D'Alembert waveguide Right: Long-Range waveguide.

1. Positive and negative group velocity, wave-stopping effects, $\chi \ll -1$

In Figure 10, the waveguide response is shown for $\chi = -100$. On the left, a wave train packet is plotted, taking a frequency bandwidth around $\Omega = 10$ and wavenumber about $k = 1.4$ (selected along the small arch of dispersion curve about A of Figure 9, i.e. in the PGV range). As it appears, positive group velocity is observed with a value that is consistent with the findings of Figure 3. On the right, another wave train is considered with same frequency bandwidth, but with wavenumbers taken on NGV branch, along a small arch about the point B. Figure 10 illustrates the negative group velocity effect. Phase wave speed has different values with respect to the group velocity and they are consistent with those predicted in Figure 4.

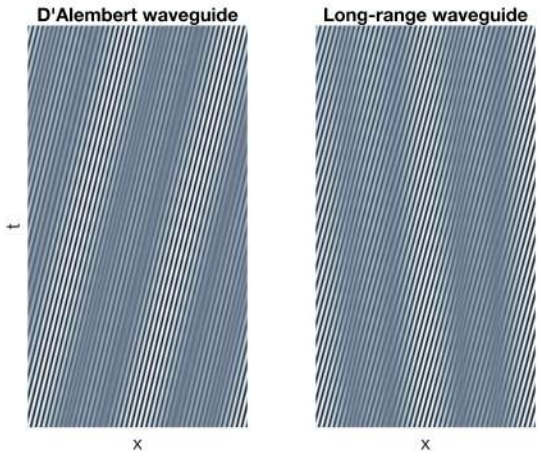

Figure 13: Surface colour plot of $w(x,t)$. Left: D'Alembert waveguide, Right: Long-Range waveguide.

Figure 11 plots the same effect, but following a different representation. Negative slope of shaded bands corresponds to negative group velocity. Phase speed characteristic lines have different (positive) slopes, anew consistently with values shown in Figure 4.
In Figures 12 and 13, a wave train packet is generated using frequencies about $\Omega = 12$ and wavenumber $K = 2$ on a small arch about the point C. The left side of Figures 12 and 13 shows standard waves, and compares with right side, revealing that long-range effect produces the waves envelope that does not propagate, providing a wave-stopping phenomenon.

2. Hypersonic effect, $\chi \gg 1$

Figure 14 (right) shows the hypersonic (superluminal) propagation of the envelope, compared with the D'Alembert case (left), in which the crest remains substantially close to the centerline. On the right, it also appears that phase velocity in the long-range case is substantially vanishing according to Figure 7c.
Figure 15 shows shaded bands with high slope and a striped texture almost horizontal for phase speed.
According to Figure 7b, Figure 15 clearly displays the hypersonic (superluminal) effect.

VI. NONLOCAL RETARDED ACTIONS

Since the group velocity can reach, in the range $\chi \gg 1$, even unbounded values (see Figure 7b), it is natural to ask if this effect is implied or related to the instantaneous propagation of the long-range forces. In fact, nonlocal elasticity assumes the force $\mathbf{F}$ acting on the particle at $\mathbf{P}(\boldsymbol{x})$ due to the particle at $\mathbf{Q}(\boldsymbol{\xi})$ is transmitted without any delay.

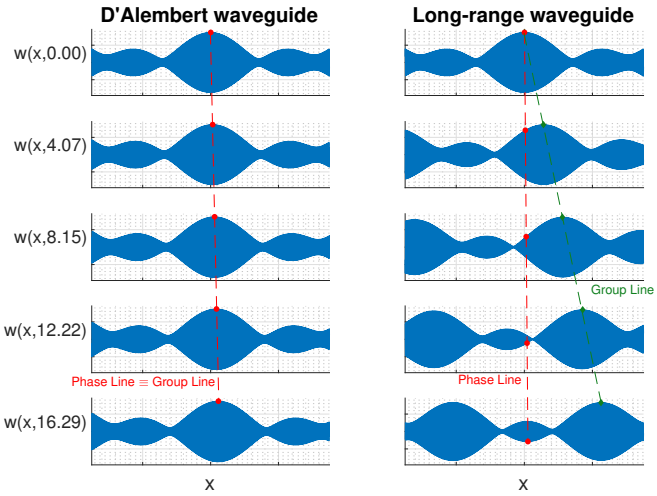

Figure 14: Hypersonic (superluminal) effect. Left: D'Alembert waveguide, Right: Long-Range waveguide.

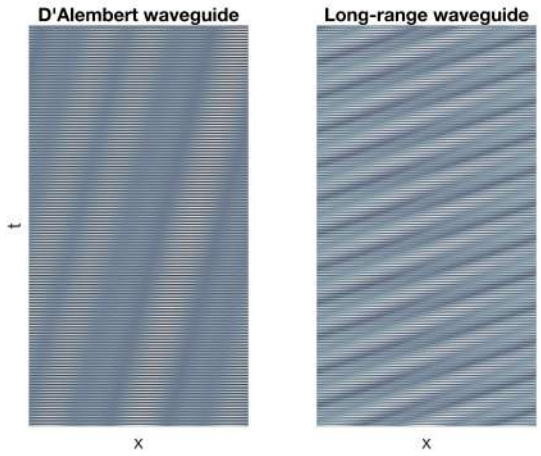

Figure 15: Surface colour plot of $w(x,t)$. Left: D'Alembert waveguide, Right: Long-Range waveguide.

Of course, in many cases, this can be a reasonable approximation when the forces are delayed of negligible times with respect to the characteristic period of oscillation of the particles.
However, simple considerations can enlighten the effect of a finite speed v_f of interaction propagation between distant particles, implying the delay $\tau = \dfrac{x-\xi}{v_f}$ of the perturbation at $\mathbf{Q}(\boldsymbol{\xi})$ to reach $\mathbf{P}(\boldsymbol{x})$. This transforms (11) in a delayed integral-differential equation:

$$\rho\frac{\partial^2 w(x,t)}{\partial t^2} - E\frac{\partial^2 w(x,t)}{\partial x^2} - g(x) * w(x,t-\tau) = 0 \quad (22)$$

After some mathematics, the Fourier transform of this equation provides:

$$\left[\rho\omega^2 - Ek^2 + G\left(k + \frac{\omega}{v_f}\right)\right] W(k,\omega) = 0 \qquad (23)$$

If the Gauss-like force is considered, the associated dispersion relationship becomes:

$$\Omega^2 - K^2 + \chi\left(K + \frac{\Omega}{V}\right)^2 e^{-\frac{\left(K+\frac{\Omega}{V}\right)^2}{4}} = 0 \qquad (24)$$

where $V = \dfrac{v_f}{c}$.
For $V \to \infty$, (24) collapses into equation (17). For $V \to 0$, the standard D'Alembert dispersion is obtained. From equation (24), it is deduced that C_g and C_φ can be both higher than V, and that C_g can be negative even for $\chi \gg 1$.

In particular, for $V = 1$, i.e. when the speed of the disturbance is comparable with the speed of sound $v_f = c$, the map of Figure 16 is obtained. A comment on the leap line $IASA'I'$. Following it from the point I (asymptotically converging over the line $\chi = 0$) to A, it identifies all the points for which $C_g \to +\infty$. From A to S, C_g has its maximum that, however, is finite. From A' to I', the line identifies all the points for which $C_g = 0$. From A' to S, C_g has its minimum (positive), and no chances of wave-stopping.

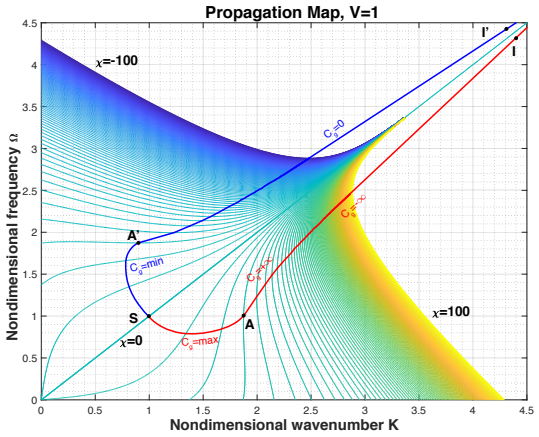

Figure 16: Group velocity and Superluminal effect for a retarded signal with $V = 1$.

VII. NOTES ON THE EFFECTS OF DISSIPATION

Historically, the discussion about superluminal effects first appeared in a seminal work of Brillouin[42] in the context of wave propagation in dissipative media, showing the appearance of group velocity that can exceed the speed of light. The previous analysis shows conversely how a loss-free elastic material but with long-range interaction, can exhibit similar superluminal effects. It is interesting to explore the combined effects of dissipation

and nonlocality, completing equation (11) with a viscous term:

$$\rho\frac{\partial^2 w}{\partial t^2}+\gamma\frac{\partial w}{\partial t}-E\frac{\partial^2 w}{\partial x^2}-g(x)*w(x)=0 \tag{25}$$

that leads to the nondimensional dispersion relationship:

$$\Omega=-\jmath\frac{\Gamma}{2}\pm\sqrt{Q^2-\left(\frac{\Gamma}{2}\right)^2} \tag{26}$$

where $\Gamma=\frac{\gamma\beta}{\sqrt{\rho E}}$, $Q^2=K^2[1-\chi\phi(K)]$ and $\phi(K)=e^{-\frac{K^2}{4}}$, $\phi(K)=\frac{8}{(K^2+1)^2}$ for the Gaussian and Laplace cases, respectively. The group velocity, in this case, becomes complex:

$$C_g=\frac{\partial\Omega}{\partial K}=\pm\frac{1}{\sqrt{1-\left(\frac{\Gamma}{2Q}\right)^2}}\frac{\partial Q}{\partial K}=\pm\frac{1}{\sqrt{1-\left(\frac{\Gamma}{2Q}\right)^2}}C_{g\Gamma=0} \tag{27}$$

in which, interestingly, the long-range and dissipation effects appear in a factorized form.

Let us analyse the two extreme cases. In the absence of dissipation, $\Gamma=0$, then $c_g=c_{g\Gamma=0}$, that is the group velocity discussed in the previous sections. In the absence of long-range interactions, $Q=K$, then $\frac{\partial Q}{\partial K}=1$ and the group velocity becomes $c_g=\pm\frac{1}{\sqrt{1-\left(\frac{\Gamma}{2Q}\right)^2}}$ that can be discussed in terms of Γ to assert superluminal effects, i.e. $c_g>1$, as in [42]. This happens for $\sqrt{1-\left(\frac{\Gamma}{2Q}\right)^2}<1$ and $\sqrt{1-\left(\frac{\Gamma}{2Q}\right)^2}$ real. When both the effects are simultaneously present, the real part of c_g can be larger or smaller than 1, depending on the choices of Γ and χ.

We conclude that in the presence of both long-range interaction and dissipation, certainly superluminality can appear. Moreover, the two effects can cooperate or compete in producing superluminal effects, depending on the considered frequency range and the intensity of both dissipation and long-range forces. As a final conclusion, dissipation is not a necessary condition to obtain superluminality. This corroborates the observations contained in [44], where the authors conclude *"...superluminal group velocity is possible...with no appreciable absorption or amplification"*.

VIII. PROPAGATION MAP AND CONCLUSIONS

The present investigation defines how long-range interactions in elastic metamaterials can produce a variety of new effects in wave propagation.

A complete theoretical analysis is presented, based on the two families of nonlocal interactions, named Gauss-like and Laplace-like, respectively. They have the merit to be rapidly decaying with the distance, to fulfill the action-reaction principle requirement, and to be available for closed form investigation of their dispersion relationships. Their general nature corroborates the idea that the properties deduced for them are representative of a general scenario expected for a large class of elastic metamaterials (and possibly for a class of long range interactions in a lattice or in charged gases).

The study is conducted embedding the long-range forces of exponential type $f(r)=\mu e^{-\left(\frac{r}{\beta}\right)^2}$ into a conventional elastic waveguide, and discussing the effect they produce, based on one single dimensionless parameter $\chi=\frac{E^*}{E}$. It takes into account the ratio of the long-range elastic modulus $E^*=\frac{\mu\beta^3}{2\sqrt{2}}$ and of the Young modulus E. E^* can be either positive or negative, depending on the attractive or repulsive nature of the interaction force.

Two opposite scenarios emerge for different values of E^*: large and negative E^* leads to wave-stopping and negative group velocity, large and positive E^* produces hypersonic (superluminal) effects, at the boundary with an unstable region. When $|E^*|$ is close to E, none of the previous effects is observed, but an eigenstate migration appears that moves the system modes from higher to lower frequency or vice versa, identifying a characteristic folding wavenumber.

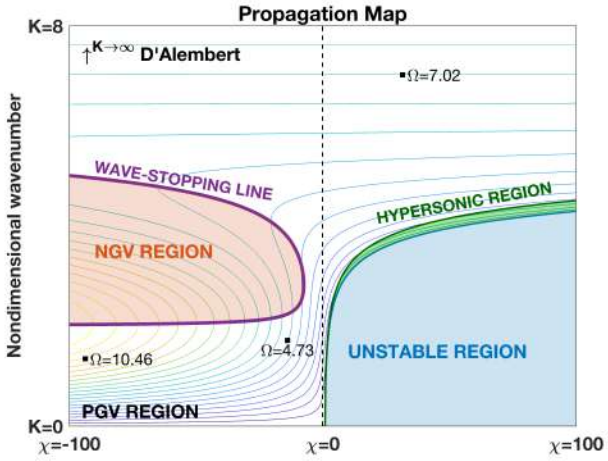

Figure 17: Propagation Map for instant long-range interaction.

A propagation map is depicted in Figure 17 (with equal-frequency contours), in which all the scenarios investigated in the present paper for $V=+\infty$ are reported for the Gauss-like case. In particular, we can identify the NGV region, bounded by the wave-stopping curve, and the unstable region, delimited by the hypersonic (superluminal) curve separating from the instability region (at $\Omega=0$).

Finally, the combined effect of retarded and long-range actions is investigated. It is shown that, even if a limit speed v_f exists for the interaction signal, still the group and phase velocity can be higher than v_f, a possibility discussed in [42].
Finally, the effect of dissipation is investigated and it has been demonstrated not crucial to obtain superluminality. Long-range elastic interaction produces superluminality even in the absence of dissipative effects.
Because of the properties of the Gauss-like force, essentially of decaying type with the distance, we can conjecture these map have a universal character in describing the expected scenarios for long-range interactions in metamaterials. Their use could represent a reference for designing new metamaterials of desired specific properties.

The theoretical presented background has wider potential uses. In fact, the long-distance interaction is a recurring challenge in physics. Statistical mechanics of complex systems is classically based on Boltzmann theory and the collision integral represents typical "short-range" interactions.
The Vlasov theory attacks long-range interaction for the evaluation of the probability density of a system of charged particles as electrons or plasma ions. Long-range thermodynamics [45] produces unusual effects as negative specific heat, anomalous diffusion, ergodicity breaking and new regimes in cold gases.
The model introduced in this paper provides, in this respect, an interpretation of deterministic effects that can be expected for long-range retarded interactions.
Beyond physics, the population dynamics has a very interesting aspect that relates to the interaction range. Recent studies in crowd dynamics [46] propose models of social forces including repulsive or attractive actions, and these models can be used to predict catastrophic scenarios [47]. Traffic modeling is one of the possibilities these models offers [48].
The mathematical model of waves generated in a population of particles, as in the presented investigation, can be interpreted as the collective behaviour of a population of individuals, the mutual interactions of which produces faster or slower social effects. The retarded action shows the effects of communication delay between pair of individuals that affects the global response of the community.

[1] Vincent Laude and Maria E Korotyaeva, "Stochastic band structure for waves propagating in periodic media or along waveguides," arXiv preprint arXiv:1801.09914 (2018).
[2] Andres D Neira, Gregory A Wurtz, and Anatoly V Zayats, "Superluminal and stopped light due to mode coupling in confined hyperbolic metamaterial waveguides," Scientific reports **5**, 17678 (2015).
[3] DE Chang, Amir H Safavi-Naeini, Mohammad Hafezi, and Oskar Painter, "Slowing and stopping light using an optomechanical crystal array," New Journal of Physics **13**, 023003 (2011).
[4] Mehmet Fatih Yanik and Shanhui Fan, "Stopping light all optically," Physical review letters **92**, 083901 (2004).
[5] Kosmas L Tsakmakidis, Tim W Pickering, Joachim M Hamm, A Freddie Page, and Ortwin Hess, "Completely stopped and dispersionless light in plasmonic waveguides," Physical review letters **112**, 167401 (2014).
[6] Dexin Ye, Yannick Salamin, Jiangtao Huangfu, Shan Qiao, Guoan Zheng, and Lixin Ran, "Observation of wave packet distortion during a negative-group-velocity transmission," Scientific reports **5**, 8100 (2015).
[7] David Maximilian Storch, Mauritz Van den Worm, and Michael Kastner, "Interplay of soundcone and supersonic propagation in lattice models with power law interactions," New Journal of Physics **17**, 063021 (2015).
[8] Jingyuan Qu, Alexander Gerber, Frederik Mayer, Muamer Kadic, and Martin Wegener, "Experiments on metamaterials with negative effective static compressibility," Physical Review X **7**, 041060 (2017).
[9] Nicolas Brunner, Valerio Scarani, Mark Wegmüller, Matthieu Legré, and Nicolas Gisin, "Direct measurement of superluminal group velocity and signal velocity in an optical fiber," Physical review letters **93**, 203902 (2004).
[10] WM Robertson, J Pappafotis, P Flannigan, J Cathey, B Cathey, and C Klaus, "Sound beyond the speed of light: Measurement of negative group velocity in an acoustic loop filter," Applied physics letters **90**, 014102 (2007).
[11] D Mugnai, A Ranfagni, and R Ruggeri, "Observation of superluminal behaviors in wave propagation," Physical review letters **84**, 4830 (2000).
[12] Michael D Stenner, Daniel J Gauthier, and Mark A Neifeld, "The speed of information in a 'fast-light'optical medium," Nature **425**, 695 (2003).
[13] B Shokri, S Kh Alavi, and AA Rukhadze, "Surface waves on a piezo-plasma-like medium," Physica Scripta **73**, 23 (2005).
[14] Carmel Rotschild, Barak Alfassi, Oren Cohen, and Mordechai Segev, "Long-range interactions between optical solitons," Nature Physics **2**, 769 (2006).
[15] Boris M Smirnov, *Fundamentals of ionized gases: basic topics in plasma physics* (John Wiley & Sons, 2012).
[16] Victor A Eremeyev, Leonid P Lebedev, and Holm Altenbach, *Foundations of micropolar mechanics* (Springer Science & Business Media, 2012).
[17] Antonio Carcaterra, F Dell'Isola, R Esposito, and M Pulvirenti, "Macroscopic description of microscopically strongly inhomogenous systems: A mathematical basis for the synthesis of higher gradients metamaterials," Archive for Rational Mechanics and Analysis **218**, 1239–1262 (2015).
[18] A Cemal Eringen, "Plane waves in nonlocal micropolar elasticity," International Journal of Engineering Science **22**, 1113–1121 (1984).
[19] A Cemal Eringen, "Linear theory of micropolar elasti-

city," Journal of Mathematics and Mechanics , 909–923 (1966).
[20] A Cemal Eringen, "Linear theory of nonlocal elasticity and dispersion of plane waves," International Journal of Engineering Science **10**, 425–435 (1972).
[21] Noël Challamel, Lalaonirina Rakotomanana, and Loïc Le Marrec, "A dispersive wave equation using nonlocal elasticity," Comptes Rendus Mécanique **337**, 591–595 (2009).
[22] Z Rueger and RS Lakes, "Strong cosserat elasticity in a transversely isotropic polymer lattice," Physical review letters **120**, 065501 (2018).
[23] Tobias Frenzel, Muamer Kadic, and Martin Wegener, "Three-dimensional mechanical metamaterials with a twist," Science **358**, 1072–1074 (2017).
[24] Daniel Torrent, Yan Pennec, and Bahram Djafari-Rouhani, "Resonant and nonlocal properties of phononic metasolids," Physical Review B **92**, 174110 (2015).
[25] Leon Brillouin, *Wave propagation in periodic structures: electric filters and crystal lattices* (Courier Corporation, 2003).
[26] Walter A Harrison, "ibid. 136, a1107 (1964)," Phys. Rev. **136**, A1107 (1964).
[27] Dionisio Del Vescovo and Ivan Giorgio, "Dynamic problems for metamaterials: review of existing models and ideas for further research," International Journal of Engineering Science **80**, 153–172 (2014).
[28] Vasily E Tarasov and George M Zaslavsky, "Fractional dynamics of coupled oscillators with long-range interaction," Chaos: An Interdisciplinary Journal of Nonlinear Science **16**, 023110 (2006).
[29] Vasily E Tarasov, "Continuous limit of discrete systems with long-range interaction," Journal of Physics A: Mathematical and General **39**, 14895 (2006).
[30] Angela Madeo, Gabriele Barbagallo, Marco Valerio d'Agostino, Luca Placidi, and Patrizio Neff, "First evidence of non-locality in real band-gap metamaterials: determining parameters in the relaxed micromorphic model," in *Proc. R. Soc. A*, Vol. 472 (The Royal Society, 2016) p. 20160169.
[31] Dexin Ye, Guoan Zheng, Jingyu Wang, Zhiyu Wang, Shan Qiao, Jiangtao Huangfu, and Lixin Ran, "Negative group velocity in the absence of absorption resonance," Scientific reports **3**, 1628 (2013).
[32] Mario Di Paola, Giuseppe Failla, Antonina Pirrotta, Alba Sofi, and Massimiliano Zingales, "The mechanically based non-local elasticity: an overview of main results and future challenges," Phil. Trans. R. Soc. A **371**, 20120433 (2013).
[33] Richard Phillips Feynman and FL Vernon Jr, "The theory of a general quantum system interacting with a linear dissipative system," Annals of physics **281**, 547–607 (2000).
[34] Francisco Jauffred, Roberto Onofrio, and Bala Sundaram, "Universal and anomalous behavior in the thermalization of strongly interacting harmonically trapped gas mixtures," Journal of Physics B: Atomic, Molecular and Optical Physics **50**, 135005 (2017).
[35] Amir O Caldeira and Anthony J Leggett, "Path integral approach to quantum brownian motion," Physica A: Statistical mechanics and its Applications **121**, 587–616 (1983).
[36] Antonio Carcaterra and A Akay, "Dissipation in a finite-size bath," Physical Review E **84**, 011121 (2011).
[37] Antonio Carcaterra and A Akay, "Fluctuation-dissipation and energy properties of a finite bath," Physical Review E **93**, 032142 (2016).
[38] A. D. Pierce, "Resonant-frequency-distribution of internal mass inferred from mechanical impedance matrices, with application to fuzzy structure theory," Journal of Vibration and Acoustics **119**, 324–333 (1997).
[39] A. A. Vlasov, "On high-frequency properties of electron gas," Journal of Experimental and Theoretical Physics **8**, 291–318 (1938).
[40] Varun D. Vaidya, Yudan Guo, Ronen M. Kroeze, Kyle E. Ballantine, Alicia J. Kollár, Jonathan Keeling, and Benjamin L. Lev, "tunable-range, photon-mediated atomic interactions in multimode cavity qed," Physical Review X **8**, 011002 (2018).
[41] Shruti Puri, Christian Kraglund Andersen, Arne L. Grimsmo, and Alexandre Blais, "quantum annealing with a network of all-to-all connected, two-photon driven kerr nonlinear oscillators," arXiv preprint arXiv:1609.07117 (2016).
[42] Léon Brillouin, *Wave propagation and group velocity*, Vol. 8 (Academic Press, 2013).
[43] Shaukat Ali Shan and Q Haque, "Low frequency electrostatic nonlinear structures in an inhomogeneous magnetized non-maxwellian electron–positron–ion plasma," Physics Letters A **382**, 99–105 (2018).
[44] L. J. Wang, A. Kuzmich, and A. Dogariu, "Erratum: Gain-assisted superluminal light propagation," Nature **406**, 277–279 (2000).
[45] Freddy Bouchet, Shamik Gupta, and David Mukamel, "Thermodynamics and dynamics of systems with long-range interactions," Physica A: Statistical Mechanics and its Applications **389**, 4389–4405 (2010).
[46] Dirk Helbing, Ansgar Hennecke, Vladimir Shvetsov, and Martin Treiber, "Micro-and macro-simulation of freeway traffic," Mathematical and computer modelling **35**, 517–547 (2002).
[47] H Gayathri, PM Aparna, and Ashish Verma, "A review of studies on understanding crowd dynamics in the context of crowd safety in mass religious gatherings," International Journal of Disaster Risk Reduction (2017).
[48] Dirk Helbing and Peter Molnar, "Social force model for pedestrian dynamics," Physical review E **51**, 4282 (1995).